Study of indentation microhardness of bismuth-doped As_2Se_3 glasses

T. KAVETSKYY[a, b], J. BORC[c*], K. SANGWAL[c]
[a]*Solid State Microelectronics Laboratory, Drohobych Ivan Franko State Pedagogical University, ul. I. Franko 24, Drohobych, 82100, Ukraine*
[b]*Institute of Materials, Scientific Research Company "Carat", ul. Stryjska 202, Lviv, 79031, Ukraine*
[c]*Department of Applied Physics, Lublin University of Technology, ul. Nadbystrzycka 38, 20-618 Lublin, Poland*

The experimental results of an investigation of the load dependence of microhardness of the surfaces of samples of $(As_{1-x}Bi_x)_2Se_3$ glasses with $x \leq 0.1$ wt fraction are described and discussed. It was observed that, with an increase in indentation diagonal d, the microhardness H_V of the samples first increases (reverse indentation size effect; reverse ISE), then decreases showing a maximum hardness H_{max} (normal ISE), and finally increases again after attaining a minimum hardness H_{min} (reverse ISE). The experimental data in the former two regions were analyzed by using the relation $H_V = H_0(1+d_0/d)$, where H_0 is the load-independent hardness of a sample and the parameter d_0 is related to elastic and plastic deformation of the sample. It was found that the load-independent H_0 for the samples initially increases up to maximum value (for $x = 0.025$) and then decreases with increasing Bi content x in these regions. These results are attributed to changes caused by Bi additive in the structure of flow defects participating in plastic deformation of the $(As_{1-x}Bi_x)_2Se_3$ samples.

(Received January 21, 2011; accepted July 25, 2011)

Keywords: Indentation microhardness, Indentation size effect, Load-independent hardness, As_2Se_3 glasses, Bismuth dopant

1. Introduction

Recently, the authors investigated [1] the load dependence of microhardness of some metal-modified arsenic chalcogenide glasses: $X_x(As_2S_3)_{100-x}$ (x = 0 or 15, and X = Ag and AgI) and As_2Se_3 without and with 0.5 at.% RE (RE = Nd, Sm, Ho and Er) in a wide range of applied indentation load. It was observed for both As_2S_3-Ag/AgI and As_2Se_3:RE (RE = Nd, Sm, Ho and Er) systems that, with an increase in indentation load P, for both systems the microhardness H_V first increases (reverse indentation size effect; reverse ISE), then decreases showing a maximum hardness H_{max} (normal ISE), and finally increases again after attaining a minimum hardness H_{min} (reverse ISE). It was suggested that, with an increase in applied load P, the initial increase in microhardness of metal-modified arsenic chalcogenide glasses up to H_{max} at small d and final increase in microhardness after H_{min} for large d are due to tensile surface stresses, while a decrease in microhardness between H_{max} and H_{min} at intermediate indentation diagonal d is due to compressive elastic surface stresses. Release of these surface stresses occurs due to elastic recovery in the near-surface layer up to d_{max} when H_{max} is attained and development of indentation cracks in the sample bulk after d_{min} when H_{min} is attained.

The above work [1] on metal-modified arsenic chalcogenide glasses is the only one where the load dependence of microhardness and the effect of known concentration of different dopants on the load-independent hardness have been investigated. Therefore, it was considered worthwhile to carry out another study on arsenic chalcogenide glasses containing different concentrations of a particular additive. The present paper reports the results of such a study on As_2Se_3 glasses containing Bi content $x \leq 0.1$ weight fraction, where the aim is (1) to investigate the nature of load dependence of microhardness of the surfaces of different samples of $(As_{1-x}Bi_x)_2Se_3$ glasses, and (2) to analyze the effect of Bi content x on the indentation size effect and load-independent hardness.

2. Experimental

The bulk $(As_{1-x}Bi_x)_2Se_3$ samples for indentation deformation were prepared by the conventional melt-quenching technique in evacuated quartz ampoules from appropriate mixtures of high purity precursors [2-4]. The amorphous state of the prepared samples was verified by x-ray diffraction analysis using the HZG-4a diffractometer (Cu K_α-radiation). From the ingots bulk samples in the form of disks of about 1–1.5 mm thickness were cut and subsequently polished using diamond paste with grain size 0.8 μm to yield high optical-quality surfaces for measurements. To remove mechanical strains developed during the synthesis, cutting and polishing procedure, the samples were annealed for 1 h at a temperature 20–30 K below the glass transition temperature. The chemical composition of the investigated samples is given in Table 1. In the paper Bi content x in different samples is given in weight fraction.

Indentation were made on the samples using Anton Paar MHT-10 hardness tester fitted to a Carl Zeiss "Axiotech" metallurgical microscope and Polaroid camera.

Loads P ranging from 0.005 to 1 N were used for indentation time of 10 s. The offset of diagonal tip was < 0.25 μm and the load resolution was 0.001 N. To avoid overlapping of surface stresses developed around neighboring indentations the separation between indentation diagonals was kept more than ten times the diagonal length of indentation impressions. The dimensions of both diagonals d made at a particular load P were measured, and the average diagonal d was calculated. The value of microhardness H_V was computed from the $P(d)$ data using the standard relation [5,6]:

$$H_V = kP/d^2, \quad (1)$$

where k is a geometrical conversion factor for the indenter used. The average values of indentation diagonal d and microhardness H_V for at least 5 indentations were used in the analysis of indentation size effect and hardness measurements. In the case of the Vickers indenter when P is taken in N and d in μm, the geometrical conversion factor k = 0.1891 and hardness H_V is in VHN (1 VHN = 9.8 MPa). The standard deviation was 5-14% from the average microhardness measured on a sample at the low loads whereas this deviation was 0.5-3% at high loads.

Typical examples of indentation imprints produced on the surfaces of $(As_{1-x}Bi_x)_2Se_3$ samples at different loads P are presented in Fig. 1. It was observed that well-defined indentations are produced on the surfaces of all samples at loads below a particular load P_c but for loads exceeding P_c radial cracks originating from the corners or in the vicinity of the corners of indentation impressions (see Fig. 1).

Table 1. Composition of investigated samples.

Sample	Chemical composition	x (wt fraction)
1	$(As_2Se_3)_{0.925}(Bi_2Se_3)_{0.075}$	0.075
2	$(As_2Se_3)_{0.95}(Bi_2Se_3)_{0.05}$	0.05
3	$(As_2Se_3)_{0.96}(Bi_2Se_3)_{0.04}$	0.04
4	$(As_2Se_3)_{0.975}(Bi_2Se_3)_{0.025}$	0.025
5	$As_2Se_3Bi_{0.0250}$	0.01235
6	$As_2Se_3Bi_{0.0050}$	0.0025
7	$As_2Se_3Bi_{0.0025}$	0.00125
8	$As_2Se_3Bi_{0.0005}$	0.00025

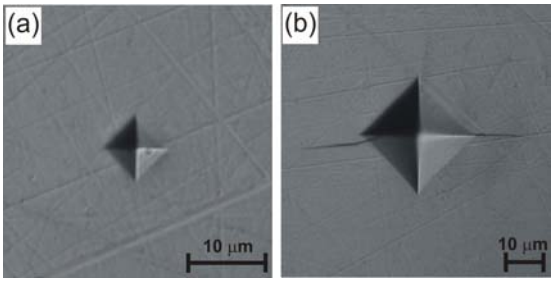

Fig. 1. Examples of indentation imprints produced on $(As_{1-x}Bi_x)_2Se_3$ samples with x = 0.05 at different loads P: (a) 0.05 N, and (b) 0.6 N.

3. Results

With an increase in load P, the microhardness H_V of $(As_{1-x}Bi_x)_2Se_3$ samples first increases, then decreases showing a maximum hardness H_{max}, and finally increases again after attaining a minimum hardness H_{min}. Fig. 2a shows examples of this behavior for samples with x = 0.00125 and 0.075. As seen from the plots in the figure, in the investigated range of applied load P one observes reverse ISE in the range of very low loads P < 0.1 N, then normal ISE in the range of intermediate loads 0.1 N < P < 0.6 N, and finally reverse ISE again in the range of high loads P > 0.6 N. The above behavior of ISEs is better revealed when the hardness data are presented as plots of microhardness H_V against indentation diagonal d, as shown in Fig. 2b for the above $(As_{1-x}Bi_x)_2Se_3$ samples and in Fig. 2c for four samples with x = 0.01235, 0.025, 0.04 and 0.05.

As reported in our previous paper [1], the dependence of microhardness of our samples may be described by the relation

$$H = H_0\left(1 + d_0 / d\right), \quad (2)$$

where the load independent hardness H_0 is the extrapolated hardness when $d^{-1} = 0$ and d_0 is a constant. The constants H_0 and d_0 are related to the nature of the investigated samples. The plots of H_V against d^{-1} for various $(As_{1-x}Bi_x)_2Se_3$ samples are shown in Fig. 3 for different regions of indentation diagonal. As found earlier [1], the experimental $H_V(d^{-1})$ data for a given sample may be fitted according to relation (2) in the three d^{-1} intervals, denoted by (I) $d^{-1} > d_{max}^{-1}$, (II) $d_{max}^{-1} > d^{-1} > d_{min}^{-1}$ and (III) $d^{-1} < d_{min}^{-1}$, with different constants H_0 and d_0. The values of the constants H_0 and d_0 in different d^{-1} intervals for various samples are listed in Table 2. As seen from Fig. 3 and Table 2, the fit is reasonably good in regions I and II.

The linear plots of measured indentation microhardness H_V against $1/d$ in regions I and II according to Eq. (2) give the values of the maximum hardness H_{max} and minimum hardness H_{min} corresponding to inverse indentation diagonals d_{max}^{-1} and d_{min}^{-1}, respectively, as listed in Table 3. The calculated values of H_{max}/H_{min} and d_{min}/d_{max} are also included in this table.

Figs. 4a and 4b show the dependence of load-independent hardness H_0 and parameter d_0, respectively, in regions I and II on Bi content x for samples. From Fig. 4a and Table 2 it may be noted that the value of H_0 for samples shows a tendency to increase with an increase in Bi content for x < 0.025 and decreases for x > 0.25 in both regions I and II. In contrast to this, as seen from Fig. 4b and Table 2, there are large errors in the average values of d_0 for different samples of Bi content x in $(As_{1-x}Bi_x)_2Se_3$ samples and it is difficult to establish an increasing or a decreasing trend of the dependence of d_0 on x in regions I and II. Therefore, it is reasonable to assume that the value of d_0 is practically constant at (0.53 ± 0.15) μm and (0.80± 0.10) μm in regions I and II, respectively, for these samples. The dependences of H_{max} and H_{min} on Bi content x for $(As_{1-x}Bi_x)_2Se_3$ samples in regions I and II (see Fig. 5)

are similar to dependences H_0 on Bi content x presented in Fig. 4a. The values of H_{max} and H_{min} are given in Table 3.

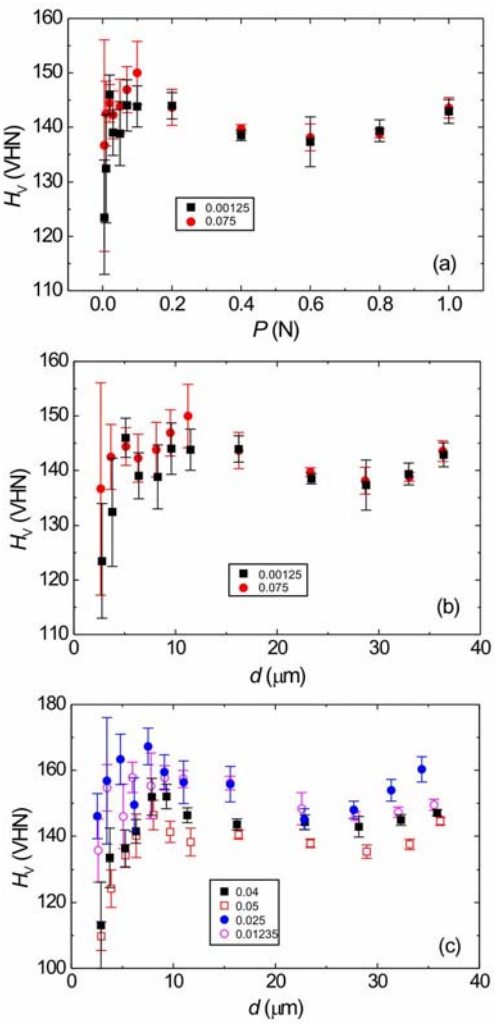

Fig. 2. Dependence of microhardness H_V on (a) applied load P for two $(As_{1-x}Bi_x)_2Se_3$ samples with x = 0.00125 and 0.075, and dependence of H_V on indentation diagonal d for (b) the above samples and (c) four samples with bismuth content x between x = 0.01235 and 0.05.

4. Discussion

Amorphous chalcogenides in the form of bulk and films show photoplastic effects [7,8], but it was argued [1] that the above-bandgap photoexposure effects will be negligible for the conditions of hardness measurements on our glass samples. To explain the indentation deformation of our glass samples one has to consider the atomic picture of their structure. One of such pictures involves the concept that localized deformable clusters of molecules, called flow defects or shear transformation zones (STZs), enable noncrystalline solids to undergo irreversible shear strains in response to applied stresses [9-11]. These flow defects (i.e. domains, clusters or STZs) are small regions, consisting of 5 to 10 molecules in special configurations, undergo inelastic rearrangement in response to shear stresses [9]. According to this concept, the curves of tensile stress as a function of strain at different temperatures and strain rates reveal a number of general features [10-12]. With increasing strain ε, the tensile stress σ at fixed strain rates first increases through a maximum at some value of strain, corresponding to yield stress, then begins to decrease and attains a steady state value, and finally material failure occurs due to shear heating and local disorder. Since the nature of the curves of Vickers hardness H_V versus indentation diagonal size d for different samples of chalcogenide glasses reported previously [1] and presented in Fig. 1 is similar to the stress–strain curves predicted theoretically by the STZ concept, it may be concluded that localized deformable clusters of molecules of glasses participate in the plastic deformation of glasses.

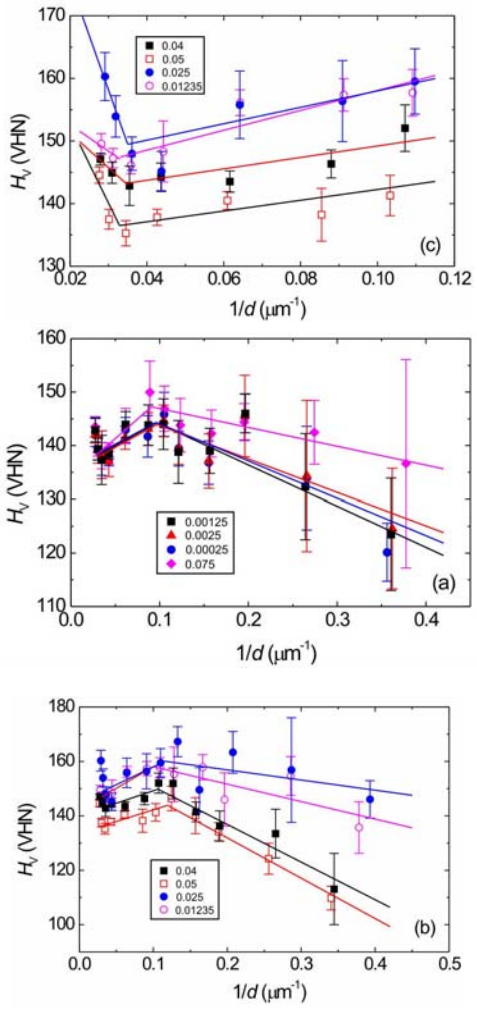

Fig. 3. Plots of H_V against d^{-1} for various $(As_{1-x}Bi_x)_2Se_3$ samples in different regions of indentation diagonal d: (a,b) I and II, and (c) II and III regions with different Bi content x.

Table 2. Values of H_0 and d_0 for different samples.

x (wt fraction)	d^{-1} interval	H_0 (VHN)	d_0 (μm)
0.00025	$d^{-1} > d_{max}^{-1}$	151.68 ± 4.43	–0.504 ± 0.130
	$d_{max}^{-1} > d^{-1} > d_{min}^{-1}$	135.38 ± 1.78	0.680 ± 0.207
	$d^{-1} < d_{min}^{-1}$	155.40 ± 7.84	–3.173 ± 1.466
0.00125	$d^{-1} > d_{max}^{-1}$	150.99 ± 3.77	–0.459 ± 0.111
	$d_{max}^{-1} > d^{-1} > d_{min}^{-1}$	135.81 ± 1.75	0.652 ± 0.203
	$d^{-1} < d_{min}^{-1}$	162.62 ± 6.54	–4.537 ± 1.116
0.0025	$d^{-1} > d_{max}^{-1}$	149.94 ± 3.64	–0.415 ± 0.109
	$d_{max}^{-1} > d^{-1} > d_{min}^{-1}$	135.14 ± 1.23	0.672 ± 0.144
	$d^{-1} < d_{min}^{-1}$	154.27 ± 6.50	–3.035 ± 1.231
0.01235	$d^{-1} > d_{max}^{-1}$	164.50 ± 4.60	–0.390 ± 0.119
	$d_{max}^{-1} > d^{-1} > d_{min}^{-1}$	142.19 ± 2.268	1.118 ± 0.247
	$d^{-1} < d_{min}^{-1}$	161.11 ± 4.27	–2.634 ± 0.762
0.025	$d^{-1} > d_{max}^{-1}$	164.37 ± 5.64	–0.227 ± 0.148
	$d_{max}^{-1} > d^{-1} > d_{min}^{-1}$	144.89 ± 3.87	0.905 ± 0.408
	$d^{-1} < d_{min}^{-1}$	210.12 ± 7.78	–8.240 ± 0.836
0.04	$d^{-1} > d_{max}^{-1}$	164.55 ± 4.32	–0.842 ± 0.110
	$d_{max}^{-1} > d^{-1} > d_{min}^{-1}$	140.07 ± 2.02	0.652 ± 0.223
	$d^{-1} < d_{min}^{-1}$	162.36 ± 2.19	–3.411 ± 0.382
0.05	$d^{-1} > d_{max}^{-1}$	161.57 ± 3.40	–0.917 ± 0.082
	$d_{max}^{-1} > d^{-1} > d_{min}^{-1}$	133.67 ± 1.70	0.641 ± 0.174
	$d^{-1} < d_{min}^{-1}$	177.74 ± 18.65	–7.062 ± 2.659
0.075	$d^{-1} > d_{max}^{-1}$	150.42 ± 1.79	–0.234 ± 0.054
	$d_{max}^{-1} > d^{-1} > d_{min}^{-1}$	134.01 ± 2.01	1.088 ± 0.239
	$d^{-1} < d_{min}^{-1}$	161.15 ± 12.93	–4.216 ± 2.247

Table 3. Values of transition d_{max}^{-1} and d_{min}^{-1} and corresponding hardness H_{max} and H_{min}

x (wt frac.)	d_{max}^{-1} (μm^{-1})	H_{max} (VHN)	d_{min}^{-1} (μm^{-1})	H_{min} (VHN)	H_{max}/H_{min}	d_{min}/d_{max}
0.00025	0.097	144.3	0.034	138.6	1.041	2.85
0.00125	0.096	144.3	0.0325	138.6	1.041	2.95
0.0025	0.097	143.5	0.034	138.3	1.037	2.85
0.01235	0.1	158.1	0.032	147.3	1.073	3.13
0.025	0.136	159.5	0.0345	149.5	1.067	3.94
0.04	0.107	148.9	0.0335	143.1	1.040	3.19
0.05	0.12	143.9	0.033	136.5	1.054	3.64
0.075	0.091	147.2	0.033	138.8	1.061	2.76

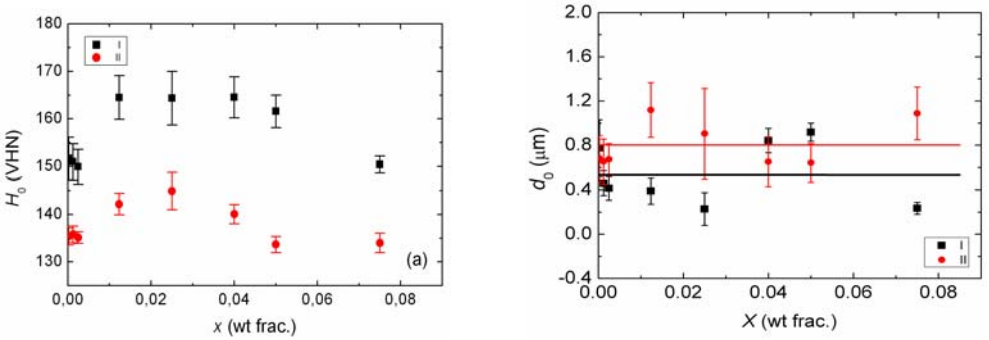

Fig. 4. Dependence of (a) H_0 and (b) d_0 in different regions on Bi content x for $(As_{1-x}Bi_x)_2Se_3$ samples.

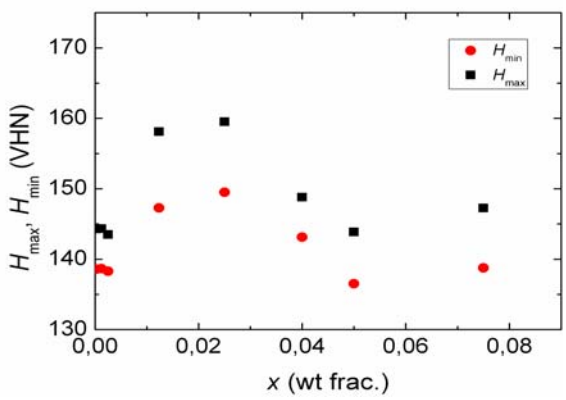

Fig. 5. Dependence of H_{max} and H_{min} on Bi content x for $(As_{1-x}Bi_x)_2Se_3$ samples.

Eq. (2) may be related to the proportional specimen resistance (PSR) model advanced by Li and Bradt [13,14]. According to this model, the ISE of a material is given by

$$P = ad + bd^2 \quad (4)$$

where the parameter a characterizes the load dependence of hardness and b is a load-independent constant. The term ad accounts for the load dependence of hardness, and the constants of Eqs. (2) and (4) are related by: $H_0 = 0.1891b$ and the constant $d_0 = a/b$. These authors [13] pointed out that the quantities a and b of Eq. (4) are related to the elastic and plastic properties of a material, respectively, and the quantity a consists of two contributions: (i) the elastic compression of the test specimen by the indenter, and (ii) the frictional resistance developed at the indenter facet/specimen interface. When elastic surface stresses are compressive, the sign of a is positive. These compressive surface stresses result in normal ISE.

Following Li and Bradt [13], we assume that the value of a is directly proportional to the above elastic contributions E for a sample and that the value of b is a measure of its load-independent hardness H. Then the ratio E/H is a measure of the magnitude of the indentation residual stresses resulting from the mismatch between the plastic zone beneath the indentation and the surrounding elastic matrix. This means that the ratio a/b may be considered as a measure of the residual stresses for a sample of given composition and is a constant quantity (i.e. $a/b = d_0 > 0$). However, as in the case of brittle compounds [15], the negative values of a suggest that the surface stresses are tensile, which implies that reverse ISE is associated with the relaxation of these surface stresses introduced by indentation (i.e. $a/b = d_0 < 0$).

Since the absolute values of d_0 (i.e. $|d_0|$) in regions I and II are practically independent of Bi content in $(As_{1-x}Bi_x)_2Se_3$ samples and $d_0 = a/b = E/H$, an increase in load-independent hardness H_0 with increasing x implies that the value of the a parameter characterizing the load dependence of their hardness also increases. This suggests that, as in the case of the dependence of H_0 on Bi content x as seen in Fig. 4a, the value of a for the samples also shows a tendency to increase with an increase for $x < 0.025$ and a decrease for $x > 0.25$ of the samples. The values of $d_0 < 0$ in regions I and III (see Table 2) also mean that $a < 0$ in these regions and is associated with tensile stresses in the surface layer. Analysis of the length c of well-defined indentation cracks as a function of applied load P for different samples indeed lends support to this inference [1]. However, the value of $d_0 > 0$ in region II implies that $a > 0$ in this region.

As seen from Table 3, irrespective of the Bi content in the samples, the values of indentation diagonals d_{max} and d_{min} are practically constant equal to 9.5 and 30.0 μm, respectively. The diagonal d_{max} corresponds to the formation of visible cracks in the surface layer of the indented samples (region I), whereas the diagonal d_{min} corresponds to the development of indentation cracks in the volume of the samples (region II). In contrast to d_{max} and d_{min}, the value of d_0 is a measure of the magnitude of the indentation residual stresses.

For Vickers indentation, indentation diagonal d and indentation depth h are related by: $d = 7h$. Therefore, the thicknesses h_{max} (= $d_{max}/7$) and h_{min} (= $d_{min}/7$) of the surface layers are 1.36 μm and 4.3 μm, respectively. This means that the surface layer in region I has a thickness of about one-half the thickness of the surface layer in region II.

As seen from Table 3, the ratios H_{max}/H_{min} and d_{min}/d_{max} are practically constant equal to 1.05 and 3.12, respectively. Consequently, as expected from the analysis of the $H_V(d)$ data, the plots of $H_0(x)$ data in regions I and II are similar to that of the plots of $H_{max}(x)$ and $H_{min}(x)$ data. These values initially increase up to a maximum at $x \approx 0.025$ and then decrease with increasing Bi content x. The observations of the changes in H_0, H_{max} and H_{min} of $(As_{1-x}Bi_x)_2Se_3$ samples in regions I and II with increasing Bi content x may be attributed to changes in the structure of flow defects participating in their plastic deformation.

Finally, it should be noted that H_{max} is higher than H_{min} by about 5% only for different samples (cf. Table 3), whereas $H_0 > H_{max}$ by about 5% in region I and $H_0 < H_{min}$ by about 2% in region II (see Tables 2 and 3). Therefore, irrespective of the region of hardness measurement, all the four quantities (i.e. H_{max}, H_{min} and two values of H_0 for regions I and II) represent the hardness of the samples. However, $H_V(d)$ data obtained on glass samples in region II provide reliable value of their true microhardness in view of small differences between calculated H_0 and H_{min} in this region.

5. Conclusions

(1) The experimental $H_V(d)$ data for different $(As_{1-x}Bi_x)_2Se_3$ samples reveal three regions of indentation diagonal d, which may be represented by linear relation (2) in the three d^{-1} intervals, denoted by (I) $d^{-1} > d_{max}^{-1}$, (II) $d_{max}^{-1} > d^{-1} > d_{min}^{-1}$ and (III)

$d^{-1} < d_{min}^{-1}$, with different constants H_0 and d_0, where H_0 is the load-independent hardness and d_0 is a measure of the residual indentation stresses for the sample. The linear plots of experimental $H_V(d^{-1})$ data in regions I and II according to Eq. (2) give the values of the maximum hardness H_{max} and minimum hardness H_{min} corresponding to inverse indentation diagonals d_{max}^{-1} and d_{min}^{-1}, respectively.

(2) The values of load-independent hardness H_0 calculated from experimental dependence of hardness H_V on indentation diagonal d in regions I and II with reference to the indented surface, the maximum hardness H_{max} from $H_V(d)$ data in region I and the minimum hardness H_{min} from $H_V(d)$ data in region II for $(As_{1-x}Bi_x)_2Se_3$ samples initially increase up to the maximum value at $x \approx 0.025$) and then decrease with increasing Bi content x. This observation is associated with changes in the structure of flow defects participating in their plastic deformation.

(3) The surface layer in region I has a thickness of about 1.36 μm while that in region II has a thickness of 4.3 μm, implying that the surface layer in region I is about one-third the thickness of the surface year in region II.

(4) The $H_V(d)$ data obtained on glass samples in region II provide reliable value of their true microhardness in view of small differences between calculated H_0 and H_{min} in this region.

References

[1] T. Kavetskyy, J. Borc, K. Sangwal, V. Tsmots, J. Optoelectron. Adv. Mater. **12**, 2082 (2010).

[2] K. Kolev, C. Popov, T. Petkova, P. Petkov, I. N. Mihailescu, J. P. Reithmaier, Sensors and Actuators B: Chemical **143**, 395 (2009).

[3] M. Iovu, S. Shutov, M. Popescu, D. Furniss, L. Kukkonen, A. B. Seddon, J. Optoelectron. Adv. Mater. **1**, 15 (1999).

[4] R. Ya. Golovchak, A. Kozdras, O. Shpotyuk, Solid State Comm. **145**, 423 (2008).

[5] B. W. Mott, Microindentation Hardness Testing, Butterworth, London (1956).

[6] H. Bückle, The Science of Hardness Testing and Its Research Applications, Ed. J. H. Westbrook and H. Conrad, ASME, Metal Park, OH, 1973, p. 453.

[7] M. L. Trunov, J. Optoelectron. Adv. Mater. **7**, 2235 (2005).

[8] M. L. Trunov, J. Optoelectron. Adv. Mater. **7**, 1223 (2005).

[9] M. L. Falk, J. S. Langer, Phys. Rev. E **57**, 7192 (1998).

[10] M. L. Falk, J. S. Langer, L. Pechenik, Phys. Rev. E **70**, 011507 (2004).

[11] J. S. Langer, Phys. Rev. E **77**, 021502 (2008).

[12] M.L. Manning, E. G. Daub, J.S. Langer, J.M. Carlson, Phys. Rev. E **79**, 016110 (2009).

[13] H. Li, R. C. Bradt, J. Mater. Sci. **28**, 917 (1993).

[14] H. Li, Y.H. Han, R. C. Bradt, J. Mater. Sci. **29**, 5641 (1994).

[15] K. Sangwal, Cryst. Res. Technol. **44**, 1019 (2009).

*Corresponding author: j.borc@pollub.pl